Title: Chronic 40-Hz LED Photobiomodulation Mitigates Oxidative Stress, Neuroinflammation, and Cognitive Impairments in a D-Galactose-Induced Aging Model

Authors: Niloofar Abedi[1], Javad Fahanik-babaei[2], Saeed Hajihashemi[1,*], Maryam Nazari[1,*]

1. *Department of Physiology, School of Medicine, Arak University of Medical Sciences, Arak, Iran .*
2. *Electrophysiology Research Center, Neuroscience Institute, Tehran University of Medical Sciences, Tehran, Iran.*

***Corresponding Author**: Maryam Nazari, Department of Physiology, School of Medicine, Arak University of Medical Sciences, Arak, Iran. Email: Maryam.nazari991@gmail.com, m.nazari@arakmu.ac.ir,
Saeed Hajihashemi, Department of Physiology, School of Medicine, Arak University of Medical Sciences, Arak, Iran. Email: s.hajihashemi@gmail.com

To appear in: **Basic and Clinical Neuroscience**

Received date: 2026/01/31

Revised date: 2026/07/13

Accepted date: 2026/07/22

Please cite this article as:

Abedi, N., Fahanik-babaei, J., Hajihashemi, S., Nazari, M. (In Press). Chronic 40-Hz LED Photobiomodulation Mitigates Oxidative Stress, Neuroinflammation, and Cognitive Impairments in a D-Galactose-Induced Aging Model. Basic and Clinical Neuroscience. Just Accepted publication Jul. 10, 2026. Doi: http://dx.doi.org/10.32598/bcn.2026.5864.1

DOI: http://dx.doi.org/10.32598/bcn.2026.5864.1

Highlights:

- 40-Hz LED therapy improved cognitive and anxiety-like behaviors in D-galactose-induced aging rats.
- 40-Hz LED therapy increased SOD activity and reduced MDA levels, restoring oxidative balance.
- 40-Hz LED therapy reduced neuroinflammation by lowering TNF-α and IL-1β level in brain tissue.
- 40-Hz LED therapy reserved hippocampal neurons and reduced neurodegeneration.

Abstract:

Background: Aging is strongly associated with oxidative stress, neuroinflammation, and cognitive decline, which collectively contribute to neurodegenerative processes. Photobiomodulation therapy (PBMT) using 40-Hz light-emitting diodes (LEDs) has emerged as a non-invasive approach with potential neuroprotective effects, but its efficacy in aging models remains insufficiently characterized.

Methods: Adult male Wistar rats were divided into control and D-galactose-treated groups, with or without 40-Hz LED exposure. Aging was induced by daily intraperitoneal injections of D-galactose (200 mg/kg) for eight weeks. PBMT was administered three times per week (15 min/session, 40 Hz). Behavioral performance was assessed using the light/dark transition and novel object recognition tests. Oxidative and inflammatory markers were analyzed by measuring superoxide dismutase (SOD) activity, malondialdehyde (MDA) content, and pro-inflammatory cytokines tumor necrosis factor-α (TNF-α) and interleukin-1β (IL-1β). Histological evaluation of hippocampal CA1 neurons was performed using hematoxylin and eosin staining.

Results: D-galactose administration induced anxiety-like behavior, impaired recognition memory, reduced SOD activity, increased MDA levels, and elevated TNF-α and IL-1β concentrations, accompanied by neuronal degeneration in the hippocampus. Chronic 40-Hz LED PBMT significantly ameliorated these effects by improving cognitive and behavioral performance, restoring antioxidant capacity, reducing neuroinflammatory cytokines, and preserving hippocampal neuronal morphology.

Conclusions: Chronic 40-Hz LED PBMT exerts potent antioxidative and anti-inflammatory effects, mitigating cognitive and histopathological alterations associated with D-galactose-induced aging. These findings suggest that 40-Hz LED PBMT represents a promising, safe, and non-invasive strategy for attenuating age-related neurodegenerative changes.

Keyword: Aging, LED therapy, photobiomodulation, oxidative stress, D-galactose, Neuroinflammation

1. Introduction

Aging represents a multifactorial biological process characterized by gradual deterioration in cellular and physiological integrity (López-Otín et al., 2023 Among all organs, the brain is particularly vulnerable to age-associated alterations, displaying progressive structural and functional impairments that underlie cognitive decline and enhance the risk of neurodegenerative disorders such as Alzheimer's disease (AD) (Almeida et al., 2017; Eikelboom et al., 2020; Mattson & Magnus, 2006). Two major contributors to brain aging are oxidative stress and the buildup of advanced glycation end products (AGEs), both of which promote neuronal dysfunction and degeneration (Aydın et al., 2016; Vina et al., 2013; Xu et al., 2016). Oxidative stress results from an imbalance between the generation of reactive oxygen species (ROS) and the antioxidant systems responsible for their removal, with mitochondria serving as a principal source and amplifier of ROS within neurons (Ionescu-Tucker & Cotman, 2021; Pak et al., 2003). Excessive ROS accumulation damages cellular macromolecules, induces DNA and membrane lipid oxidation, and activates apoptotic signaling pathways, ultimately impairing neuronal survival and cognition (Aydın et al., 2016; Xu et al., 2016). Due to its high oxygen consumption, abundant lipid content, and limited antioxidant capacity, the brain is particularly prone to oxidative injury (Çakatay, 2010). In experimental research, prolonged exposure to D-galactose—a reducing sugar implicated in AGE formation—elicits oxidative stress, inflammation, and apoptosis, reproducing key aspects of the natural aging process (Chen et al., 2015; Chen et al., 2018; Islam, 2017; Turgut et al., 2016). Therefore, D-galactose-treated rodents are commonly utilized as a reliable experimental model to study anti-aging interventions and neuroprotective strategies (Sadigh-Eteghad et al., 2017).

Elucidating the molecular and cellular mechanisms underlying brain aging is essential for designing effective preventive and therapeutic strategies to counteract its detrimental consequences. Several studies have demonstrated that antioxidant-based interventions can mitigate oxidative damage and neurodegeneration associated with aging (Chen et al., 2018; Nam et al., 2019). Among the non-invasive and non-pharmacological approaches, photobiomodulation (PBM) therapy—employing low-intensity lasers or light-emitting diodes (LEDs) within the wavelength range of approximately 600–1072 nm—has

gained growing attention for its neuroprotective potential. Despite accumulating evidence, the precise mechanisms mediating PBM's beneficial effects remain incompletely understood (Hamblin, 2016; Vatansever & Hamblin, 2012). A prevailing hypothesis proposes that PBM acts primarily through the absorption of light energy by mitochondrial chromophores, particularly cytochrome c oxidase (CCO), which enhances mitochondrial activity and modulates neuronal metabolism in a wavelength-dependent manner (Hamblin, 2016, 2019; Rojas & Gonzalez-Lima, 2013; Salehpour et al., 2019). Supporting this concept, a recent investigation demonstrated that transcranial laser stimulation at 810 nm improved spatial learning and memory in naturally aged (20-month-old) rats. This improvement was accompanied by a shift in neuroinflammatory signaling, notably reflected by decreased interleukin-5 (IL-5) levels in aged rats relative to young controls (Cardoso, de Souza Oliveira Tavares, et al., 2022).

The wavelength applied in laser or LED systems represents a major determinant of photobiomodulation efficacy. Recent findings also indicate that the mode of light delivery—specifically, pulsed versus continuous stimulation—can markedly influence the therapeutic outcomes of photobiomodulation (Hashmi et al., 2010). In several transgenic mouse models of Alzheimer's disease (Iaccarino et al., 2016; Singer et al., 2018), and in experimental paradigms of amyloid-β (Nazari, Jafari, et al., 2022; Nazari, Vajed-Samiei, et al., 2022) or streptozotocin-induced neurotoxicity (Barzegar Behrooz et al., 2024; Soleimani et al., 2024), exposure to LED light pulsed at 40 Hz within the visible spectrum (390–700 nm) has been shown to lower Aβ burden, modulate reactive oxygen species (ROS) production, and improve mitochondrial performance. These cellular and biochemical effects have collectively been linked to enhanced learning and memory functions. Despite this growing body of evidence, the potential impact of chronic 40-Hz LED stimulation on behavior and cognition in a D-galactose-induced model of aging has not yet been explored. Therefore, this study aimed first to determine whether 40-Hz LED photobiomodulation could modify behavioral and cognitive outcomes in D-galactose-treated rats. The second objective was to assess whether potential behavioral changes were accompanied by alterations in oxidative stress markers—namely superoxide dismutase (SOD) activity and malondialdehyde (MDA) levels—and inflammatory mediators such as tumor necrosis factor-α (TNF-α) and interleukin-1β (IL-1β). Furthermore, hippocampal morphology was

examined using hematoxylin and eosin (H&E) staining to evaluate potential neuroprotective effects induced by 40-Hz LED exposure.

2. Material and Methods

2.1. Animals

Male Wistar rats weighing 230–260 g were maintained under standard laboratory conditions at a controlled temperature of 22 ± 2 °C and relative humidity of 50 ± 10%, with a 12-hour light/dark cycle. The animals had free access to standard pellet diet and tap water throughout the study. All experimental procedures complied with the National Institutes of Health (NIH) Guide for the Care and Use of Laboratory Animals and received approval from the Research and Ethics Committee of Arak University of Medical Sciences (IR.ARAKMU.AEC.1403.021).

2.2. Experimental Groups and Preparation of D-galactose-Treated Rats

D-galactose (D-gal; Sigma–Aldrich, St. Louis, MO, USA) was dissolved in 0.9% saline and administered intraperitoneally (200 mg/kg/day) for 8 consecutive weeks to induce an experimental model of aging (Chen et al., 2018; Sadigh-Eteghad et al., 2017). Control animals received an equivalent volume of saline. Simultaneously, rats in the LED-treated groups were exposed to 40-Hz LED light for 15 minutes, three times per week, throughout the same 8-week period. A total of forty male Wistar rats were randomly assigned to four experimental groups:

1) Saline (Control): Received IP saline injection without light exposure, 2) Saline + Light (Saline + L): Received IP saline injection and 40-Hz LED exposure, .3) D-galactose (D-gal): Received IP D-galactose injection without light exposure, and 4) D-galactose + Light (D-gal + L): Received IP D-galactose injection and 40-Hz LED exposure.

Twenty-four hours after the final LED session, behavioral assessments were conducted, beginning with the light/dark transition (LDT) test followed by the novel object recognition (NOR) test. After behavioral testing, rats were anesthetized using ketamine (100 mg/kg) and xylazine (10 mg/kg). The whole brains were

then removed; a subset (n = 4 per group) was stored at −80°C for biochemical assays of oxidative stress and inflammatory markers, while another subset (n = 3 per group) was fixed in 10% formalin for histological examination (H&E staining). The overall experimental timeline is illustrated in Figure 1.

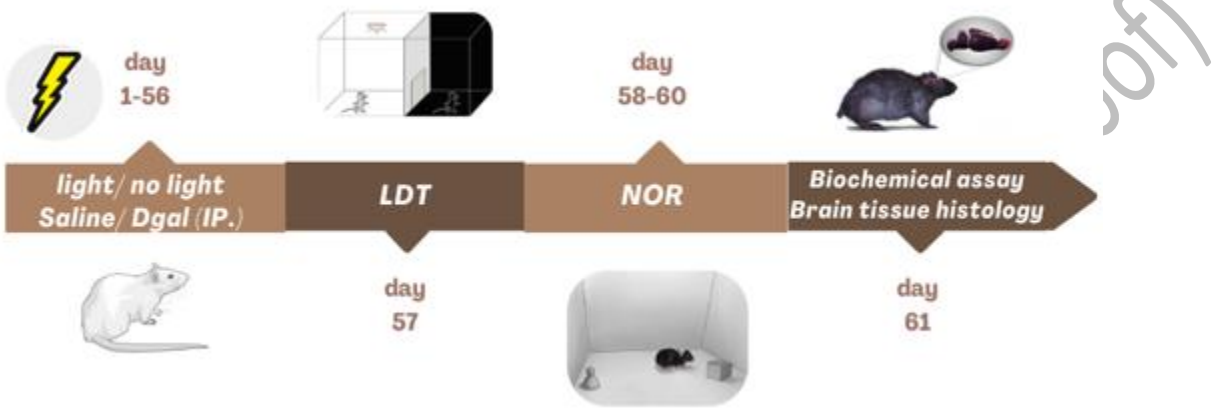

Figure 1. Experimental timeline.

2.3. LED Exposure Apparatus

As previously described (Nazari, Vajed-Samiei, et al., 2022), the setup for photobiomodulation therapy (PBMT) comprised a black box measuring 50 × 50 × 50 cm, with LED strip lights affixed to the upper interior surface (a custom-built apparatus). White LEDs (425–550 nm) were utilized, emitting an average irradiance of 12 mW/cm² and pulsed at 40 Hz. The 40-Hz pulsed light corresponds to cycles of 12.5 ms "on" and 12.5 ms "off." The modulation of light was regulated by an AVR microcontroller circuit interfaced with a computer via a USB connection.

2.4. Light/Dark test (LDT)

Anxiety-like behavior was assessed using the light/dark transition (LDT) apparatus (Fig. 2A), which consisted of two compartments connected by an open doorway. One compartment was made of opaque

black plastic, while the other was constructed of transparent plastic to create a brightly illuminated chamber. Each rat was gently placed in the light compartment at the start of the test (360 lux, provided by a 60 W bulb). The apparatus allowed free movement between the two chambers during a 5-minute trial. Anxiety-related behavior was evaluated by recording both the number of transitions into the light compartment and the total time spent there.

2.5. Novel Object Recognition (NOR) test

The Novel Object Recognition (NOR) paradigm was employed to evaluate recognition memory in rats based on their natural tendency to explore unfamiliar objects (Fig. 3A) (Rostami et al., 2024). The procedure consisted of three sequential stages: habituation, familiarization, and testing. During the habituation session, each animal was placed individually into an empty open-field box for 10 minutes to freely explore and adapt to the environment. After 24 hours, in the familiarization phase, two identical objects (A1 and A2)—identical in size, color, and material—were positioned in opposite corners of the arena, each 10 cm from the walls. Rats were then introduced facing the side opposite the objects and allowed to explore for 10 minutes. Following another 24-hour interval, one of the familiar objects was substituted with a new object (B) that differed in shape and texture (Antunes & Biala, 2012). To prevent olfactory bias, both the chamber and objects were thoroughly cleaned with 70% ethanol between sessions. Exploratory activity was recorded by a video camera positioned above the arena and analyzed using EthoVision XT software (Noldus IT, USA).

Exploration was defined as the time spent sniffing or touching the object within a 1 cm distance.

Recognition memory was quantified using two indices:

1) The **discrimination index** (DI) = [(B – A) / (A + B)] × 100
2) The **novel object index** (NOI) = (B / (A + B)) × 100

Where *A* represents the time spent exploring the familiar object, and *B* indicates the time spent exploring the novel one.

2.6. Biochemical analysis

Twenty-four hours after completion of the NOR test, the rats were deeply anesthetized and rapidly decapitated using a guillotine. Brains were promptly removed, and whole-brain tissue samples were homogenized in lysis buffer with a high-speed homogenizer. The homogenates were centrifuged at 12,000 × g for 10 min at 4 °C, and the resulting supernatants were stored at −80 °C until biochemical assessment. Total protein concentrations were determined using the Bradford method (Bradford, 1976).

Determination of MDA content:

Malondialdehyde (MDA), a well-recognized indicator of lipid peroxidation and oxidative stress, was measured using a commercial kit (Teb Pazhouhan Razi, Iran) according to the supplier's protocol. Briefly, the tissue supernatant was mixed with trichloroacetic acid (TCA) and thiobarbituric acid (TBA) reagents and heated in a water bath at 100 °C for 1 hour. After cooling, samples were centrifuged (10,000 × g, 10 min, 4 °C), and the absorbance of the clear supernatant was read at 532 nm using a spectrophotometer. MDA concentration was expressed as µmol per milligram of protein.

Determination of superoxide dismutase (SOD) activity

SOD activity was analyzed with a commercial kit (Nasdox™, Iran). Following incubation for 5 min at room temperature in darkness, optical density (OD) was recorded at 405 nm using a microplate reader. Enzyme activity was expressed as units per milligram of protein (U/mg). The principle of the assay is based on the ability of SOD to inhibit pyrogallol auto-oxidation, and the degree of inhibition was used to calculate the enzyme activity relative to the control lacking SOD.

Determination of tumor necrosis factor-α (TNF-α) and interleukin-1β (IL-1β)

Tissue concentrations of TNF-α and IL-1β were determined using commercial enzyme-linked immunosorbent assay (ELISA) kits (Sigma-Aldrich, USA; MyBioSource, USA), following the manufacturers' instructions. The absorbance of each well was recorded at 450 nm with a microplate reader,

and cytokine levels were normalized to total protein content. Final values were expressed as picograms per milligram of tissue protein (pg/mg).

2.7. Histology: Hematoxylin and Eosin (H&E) staining

After completion of behavioral testing, animals were euthanized, and brains were immersed in 10% neutral-buffered formalin for fixation. Standard histological procedures were then applied, and coronal sections (6 µm thick) were cut from paraffin-embedded brain blocks using a rotary microtome (Leica, Germany). The sections were stained with hematoxylin and eosin (H&E) and examined under a light microscope (Olympus, Japan). Representative micrographs were captured with a digital camera attached to the microscope for documentation and morphological analysis.

3. Statistical analysis

All statistical analyses were performed using GraphPad Prism software. Data distribution normality was verified using the Shapiro–Wilk test. Group comparisons were made by one-way analysis of variance (ANOVA) followed by Tukey's post hoc test for multiple comparisons. Results are presented as mean ± standard error of the mean (SEM), and statistical significance was defined as $P < 0.05$.

4. Results

4.1. Light/dark test (LDT)

One-way ANOVA analysis (Fig. 2) revealed that rats subjected to D-galactose administration for 8 weeks (Dgal group) exhibited a significant decrease in both the time spent in the light compartment ($P < 0.0001$, Fig. 2B) and the number of entries into the light compartment ($P < 0.001$, Fig. 2C) compared with the saline group. Remarkably, 40-Hz LED stimulation in D-galactose-treated rats (Dgal + L group) significantly increased the time spent in the light compartment ($P < 0.01$, Fig. 2B) and the number of entries ($P < 0.05$, Fig. 2C) relative to the Dgal group. Furthermore, no significant differences were detected between the saline

and saline + light groups in either parameter, indicating that 40-Hz light exposure alone does not alter baseline anxiety-like behavior.

These results suggest that chronic 40-Hz LED therapy attenuates anxiety-like behavior induced by D-galactose administration in aged rats.

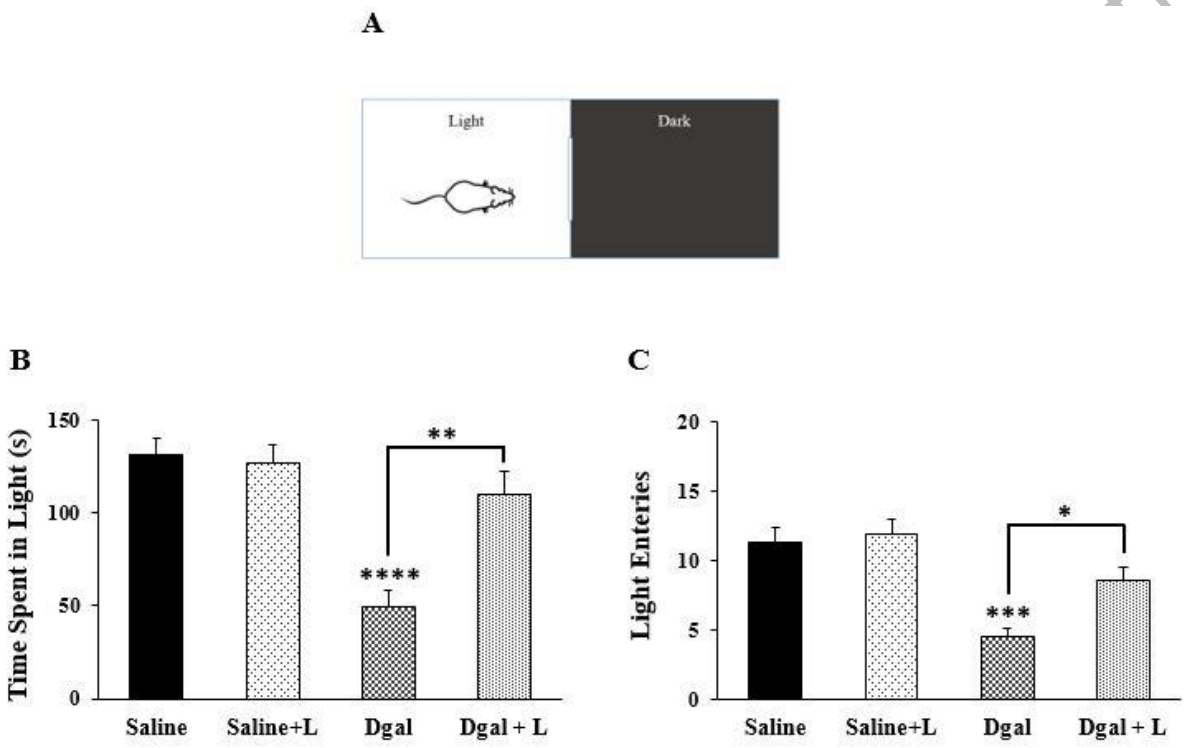

Figure 2. Effects of 40Hz light exposure on anxiety-like behavior in D-galactose-induced aged rats.

(A) Schematic of light/dark test (LDT) apparatus. One-way ANOVA revealed that D-galactose administration (Dgal group) significantly reduced (B) the time spent and (C) entries into the light compartment compared to the saline group. Notably, 40 Hz LED light exposure (Dgal + L group) reversed these effects relative to the Dgal group. No significant differences were observed between the saline and saline + light groups. Data are mean ± SEM, *P < 0.05, **P < 0.01, ***P < 0.001, ****P < 0.0001.

4.2. Novel Object Recognition (NOR) test

The Novel Object Index (NOI) and Discrimination Index (DI) were employed as quantitative indicators of recognition memory (Fig. 3). To confirm that the observed differences during the testing phase reflected memory performance rather than inconsistencies in initial object engagement, the total exploration time during the familiarization phase was analyzed. No significant variation was detected among groups ($P > 0.05$, Fig. 3B). In the testing session, one of the identical objects was substituted with a novel one to evaluate recognition memory. Statistical analysis using one-way ANOVA revealed significant intergroup differences in both the NOI (Fig. 3C) and DI (Fig. 3D). Post hoc Tukey analysis showed that the D-galactose-treated group (Dgal) displayed markedly lower exploration of the novel object, reflected by significant reductions in NOI ($P < 0.001$, Fig. 3C) and DI ($P < 0.001$, Fig. 3D) relative to the saline group. Remarkably, exposure to 40-Hz LED light (Dgal + L group) substantially improved these deficits, resulting in elevated NOI ($P < 0.01$, Fig. 3C) and DI ($P < 0.01$, Fig. 3D) compared to the Dgal group. Moreover, no significant difference was observed between the saline and saline + light (Saline + L) groups in either parameter.

Collectively, these findings indicate that chronic D-galactose exposure impairs recognition memory, as evidenced by decreased discrimination between familiar and novel objects. Treatment with 40-Hz LED light mitigated these impairments, suggesting its potential to restore or enhance cognitive performance in aging rats. The lack of behavioral alterations in the saline + L group implies that photic stimulation alone does not modify baseline recognition memory.

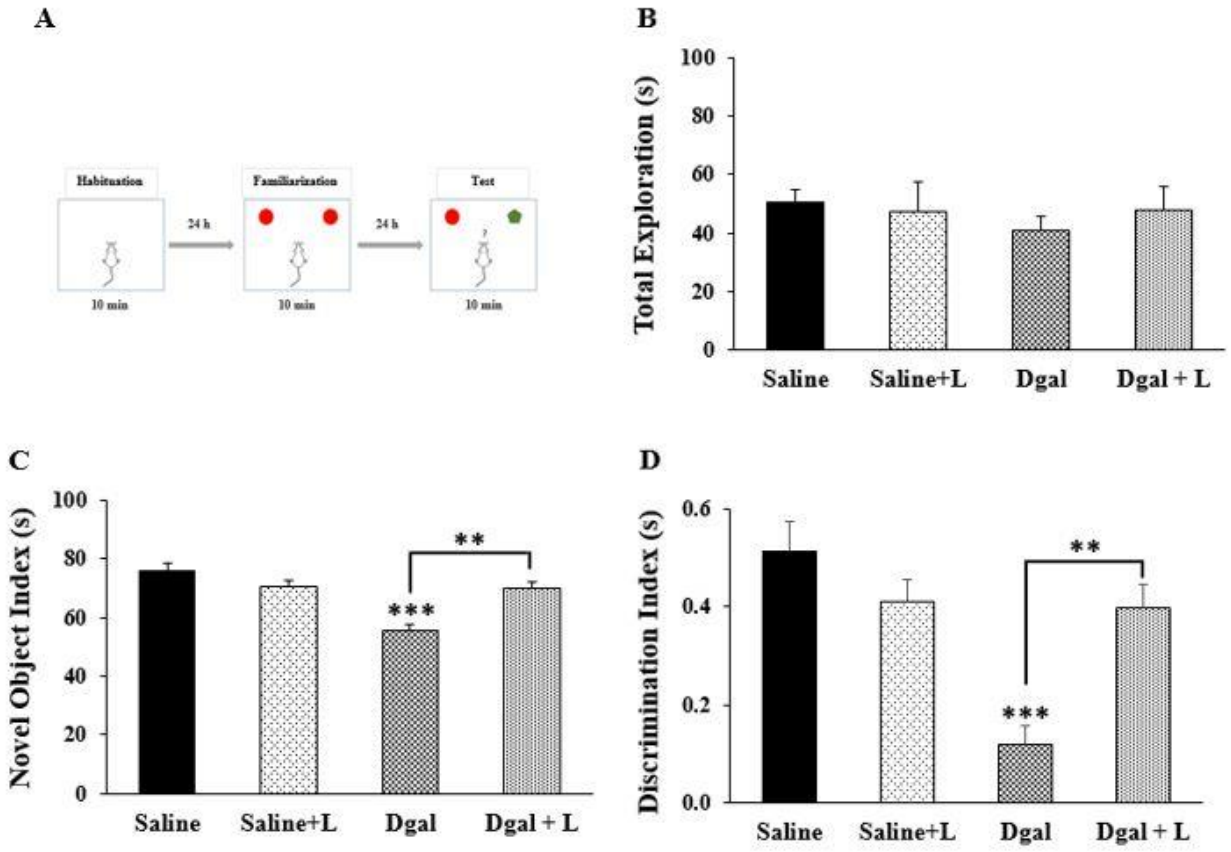

Figure 3. Effects of 40Hz light exposure on recognition memory in D-galactose-induced aged rats. (A) Schematic of Novel Object Recognition (NOR) test apparatus. (B) Total exploration time during the training session showed no significant differences among groups. (C) Novel Object Index (NOI) and (D) Discrimination Index (DI) were significantly reduced in the Dgal group compared to saline controls, indicating impaired recognition memory. Exposure to 40 Hz LED light (Dgal + L group) significantly improved both indices. No significant differences were observed between the saline and saline-light treated groups. Data are presented as mean ± SEM; one-way ANOVA, $^{**}P < 0.01$, $^{***}P < 0.001$.

4.3. Oxidative stress marker: Malondialdehyde (MDA) content and SOD activity

Substantial evidence highlights oxidative stress as a central mechanism driving cellular and neural aging (Maldonado et al., 2023). Superoxide dismutase (SOD), a key enzymatic antioxidant, represents one of the first lines of defense against reactive oxygen species (ROS)-induced damage (Demirci-Çekiç et al., 2022).

As presented in Fig. 4A, the D-galactose-treated animals (Dgal group) showed a marked decline in SOD activity compared with the saline-treated controls ($P < 0.0001$). Interestingly, exposure to 40-Hz LED light (Dgal + L group) significantly counteracted this reduction ($P < 0.01$), restoring SOD activity toward near-normal levels.

Conversely, malondialdehyde (MDA)—a robust indicator of ROS-induced lipid peroxidation (Demirci-Çekiç et al., 2022)— was markedly elevated in the brains of D-galactose-treated rats compared with saline controls ($P < 0.0001$, Fig. 4B). Treatment with 40-Hz LED light markedly diminished MDA levels ($P < 0.0001$) relative to the Dgal group, indicating mitigation of oxidative damage. Because behavioral analysis revealed no significant differences between saline and saline + light (Saline + L) groups, the latter was excluded from subsequent biochemical analyses involving oxidative and inflammatory markers.

Overall, these data indicate that chronic 40-Hz LED therapy effectively restores redox homeostasis and mitigates oxidative stress, a major contributor to neuronal dysfunction and age-related physiological decline.

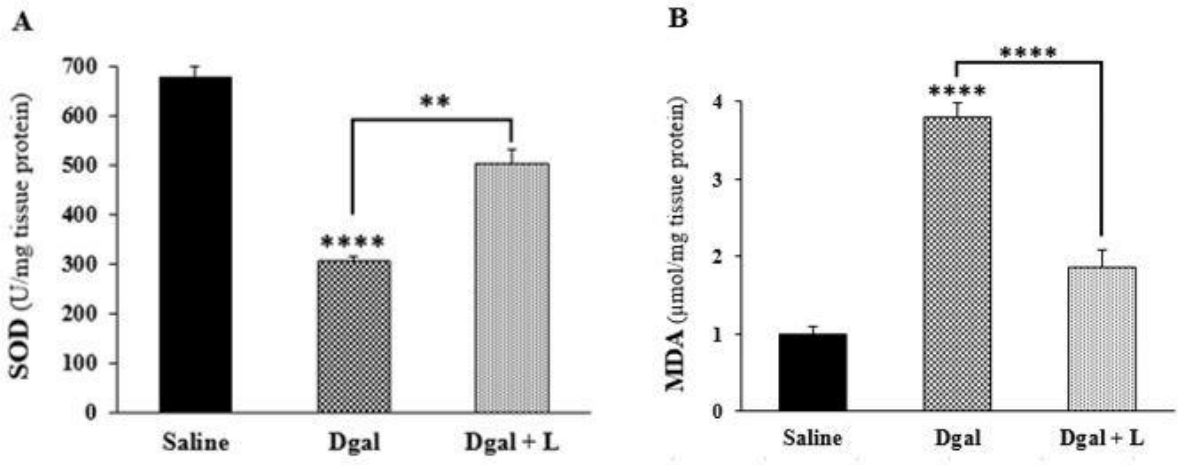

Figure 4. Effects of 40 Hz light exposure on oxidative stress markers in the brains of D-galactose-induced aged rats. (A) Superoxide dismutase (SOD) activity was significantly reduced in the Dgal group compared to saline group and was partially restored by 40Hz LED light exposure (Dgal + L group). (B) Malondialdehyde (MDA) levels were significantly elevated in the Dgal group, indicating increased lipid peroxidation, and were significantly reduced by 40 Hz light treatment. Data are presented as mean ± SEM; **P < 0.01, ****P < 0.0001.

4.4.Inflammatory cytokines: Interleukin-1β (IL-1β) and Tumor necrosis factor-α (TNF-α)

Analysis of inflammatory mediators demonstrated a pronounced increase in pro-inflammatory cytokines within the brain tissue of D-galactose-treated rats. As shown in Fig. 5A and 5B, IL-1β ($P < 0.0001$) and TNF-α ($P < 0.0001$) concentrations were markedly elevated in the Dgal group compared with the saline controls, reflecting a robust neuroinflammatory response induced by chronic D-galactose administration. Importantly, treatment with 40-Hz LED light (Dgal + L group) significantly alleviated these alterations, resulting in a substantial reduction in both IL-1β ($P < 0.0001$) and TNF-α ($P < 0.01$) levels relative to untreated D-galactose rats.

Collectively, these results indicate that chronic exposure to 40-Hz LED light exerts potent anti-inflammatory effects in the aging brain, effectively counteracting D-galactose-induced neuroinflammation.

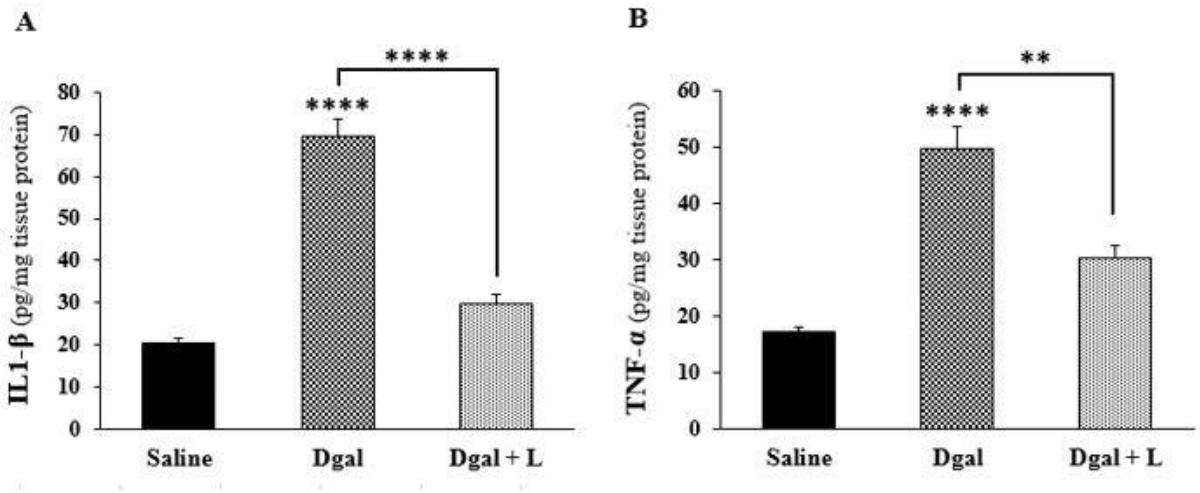

Figure 5. Effects of 40 Hz light exposure on pro-inflammatory cytokine levels in the brains of D-galactose-induced aged rats. One-way ANOVA revealed that D-galactose treatment significantly increased levels of IL-1β (A) and TNF-α (B) compared to the saline group, indicating neuroinflammation. These elevations were significantly attenuated by 40 Hz LED light exposure in Dgal + L group respect to the Dgal group. Data are presented as mean ± SEM; **$P < 0.01$, ****$P < 0.0001$.

4.5. Hematoxylin and Eosin (H&E) staining

Histopathological examination of the hippocampal CA1 region (Fig. 6) revealed clear morphological alterations across the experimental groups. In D-galactose-treated rats (Dgal group), a substantial increase in pyknotic neurons (yellow arrows) accompanied by a marked reduction in the density of intact pyramidal neurons (black arrows) was observed when compared with the saline controls, suggesting neuronal degeneration associated with aging.

Conversely, animals receiving 40-Hz LED light treatment (Dgal + L group) exhibited a noticeable reduction in neuronal loss and structural abnormalities within the CA1 region relative to the Dgal group. Nevertheless, neuronal integrity and cytoarchitectural organization were not completely restored to the level observed in control animals. These observations were derived from qualitative histological assessments without quantitative neuron counting. Representative micrographs were obtained from H&E-stained sections using a light microscope at 100× magnification.

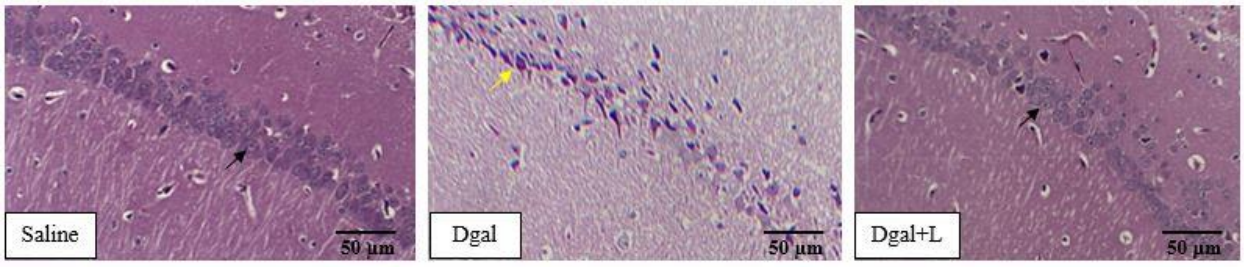

Figure 6. Effects of 40 Hz light exposure on morphological alterations in the CA1 region of the hippocampus in D-galactose-induced aging rats. Aging induction with D-galactose led to a marked increase in pyknotic neurons (indicated by yellow arrows) and a decrease in the density of pyramidal neurons with normal morphology (indicated by black arrows) compared to the saline group. Treatment with 40-Hz LED light in aged rats (Dgal+L group) resulted in a partial improvement in these pathological morphological changes relative to the Dgal group. Images were captured at 100× magnification using a light microscope.

5. Discussion

This study evaluated the therapeutic potential of 40-Hz LED photobiomodulation therapy (PBMT) in a D-galactose-induced aging rat model by comprehensively assessing behavioral performance (using the LDT

and NOR tests), oxidative stress biomarkers (SOD and MDA), inflammatory mediators (IL-1β and TNF-α), and histopathological alterations in brain tissue. The results demonstrate that chronic exposure to 40-Hz LED light markedly mitigates aging-related impairments, as reflected by improved behavioral and cognitive outcomes, decreased oxidative and inflammatory markers, and reduced neuronal degeneration.

D-galactose (Dgal) administration is a well-established model for inducing accelerated aging in rodents, as it reproduces key characteristics of natural aging, including oxidative stress, chronic inflammation, and cognitive deterioration (Chen et al., 2018; Sadigh-Eteghad et al., 2017). D-galactose promotes excessive production of reactive oxygen species (ROS) via auto-oxidation and the generation of advanced glycation end products (AGEs), which together drive oxidative damage. The resultant ROS burden overwhelms antioxidant defenses such as superoxide dismutase (SOD) and glutathione peroxidase, leading to cellular injury. Mitochondria play a central role in this cascade, as D-galactose disrupts mitochondrial function, reduces ATP synthesis and membrane potential, and amplifies ROS generation. This self-perpetuating oxidative cycle contributes to cellular dysfunction and apoptosis. Additionally, mitochondrial impairment triggers the release of pro-apoptotic factors and mitochondrial DNA, which further activate inflammatory signaling and promote neuronal loss (Islam, 2017; Jin & Cai, 2023; López-Otín et al., 2023; Sadigh-Eteghad et al., 2017). These molecular disruptions manifest as behavioral deficits in learning and memory, commonly observed in aging models (Speisman et al., 2013). In agreement with earlier findings, study also revealed that D-galactose administration elevated oxidative markers (MDA), decreased SOD activity, and increased levels of TNF-α and IL-1β. These biochemical changes correlated with anxiety-like and cognitive deficits observed in behavioral assays, together with histological evidence of neuronal degeneration, most likely resulting from oxidative and inflammatory injury.

Photobiomodulation (PBM) therapy, involving the use of low-level laser or LED light on biological tissues, has emerged as a promising non-pharmacological approach for disorders such as depression, stroke, and neurodegenerative diseases, including Alzheimer's disease (AD) and Parkinson's disease (PD) (Cardoso, Salehpour, et al., 2022; Hamblin, 2016, 2019; Schiffer et al., 2009).]. PBM offers several advantages, including affordability, safety, non-invasiveness, and ease of application (Hamblin, 2019; Rojas &

Gonzalez-Lima, 2013). For instance, transcranial near-infrared laser therapy (810 nm) has demonstrated significant neuroprotective effects in D-gal/$AlCl_3$-induced neurodegenerative models, likely mediated by the suppression of neuroinflammation and enhancement of synaptic marker expression (Hosseini et al., 2022). Likewise, 660-nm LED irradiation has been shown to counteract H_2O_2-induced oxidative stress and enhance the survival of hippocampal HT-22 cells through the upregulation of antioxidant enzymes such as glutathione peroxidase and SOD (Heo et al., 2019).

Compared with lasers, LEDs offer broader illumination and lower thermal output, making them particularly suitable for larger tissue coverage (Hamblin, 2016; Rojas & Gonzalez-Lima, 2013). Singer et al. reported that 40-Hz flickering white light substantially reduced amyloid-β (Aβ) accumulation—a hallmark of AD—indicating potential therapeutic relevance for flicker light stimulation (Singer et al., 2018). In the present study, whole-body 40-Hz LED exposure for 15 minutes, administered three times weekly for eight weeks, produced notable neuroprotective outcomes in D-galactose-treated rats. LED therapy significantly attenuated oxidative stress by reducing MDA levels and restoring antioxidant enzyme activity (SOD). It also decreased pro-inflammatory mediators, including TNF-α and IL-1β. Histological evaluations revealed preservation of hippocampal structure and decreased neuronal degeneration, in parallel with behavioral improvements in anxiety and recognition memory.

Mitochondrial function appears to be a key mechanism underlying both D-galactose-induced neurodegeneration and PBMT-mediated neuroprotection. Mitochondria are critical regulators of energy metabolism, calcium buffering, and redox balance (Casanova et al., 2023; Godoy et al., 2021). Dysregulation of these functions during aging results in decreased ATP production, excessive ROS generation, and activation of apoptotic and inflammatory pathways (Bartman et al., 2024; Casanova et al., 2023; Godoy et al., 2021; Islam, 2017, Sun et al., 2016). Elevated ROS levels can further stimulate pro-inflammatory cascades, including NF-κB and NLRP3 inflammasome activation, thereby aggravating neuronal injury (Islam, 2017; Sun et al., 2016).

In this study, elevated MDA and suppressed SOD activity confirmed the oxidative imbalance induced by D-galactose. Concurrent increases in TNF-α and IL-1β indicated persistent inflammation. PBMT

effectively counteracted these changes, suggesting its capacity to restore mitochondrial redox homeostasis and regulate inflammatory signaling. The established mechanism of PBMT involves activation of cytochrome c oxidase within the mitochondrial respiratory chain, leading to enhanced ATP synthesis and reduced ROS generation (Hamblin, 2016; Karu, 1999). Supporting this, other previous work demonstrated that 40-Hz LED exposure promotes activity of respiratory complexes I and IV and modulates mitochondrial potassium channel dynamics—key factors in mitochondrial stability and ROS regulation (Nazari, Jafari, et al., 2022; Nazari, Vajed-Samiei, et al., 2022). PBMT has also been shown to stabilize mitochondrial membranes, prevent release of damage-associated molecular patterns (DAMPs), and inhibit pro-inflammatory signaling (De Freitas & Hamblin, 2016). The observed normalization of oxidative and inflammatory markers in the present study supports these mechanisms, suggesting that PBMT restores cellular redox equilibrium and mitigates inflammation, thereby protecting vulnerable neurons.

While these findings are promising, several limitations must be acknowledged. The mechanistic interpretations are primarily based on biomarker alterations rather than direct molecular analyses. Further studies incorporating gene and protein expression profiling are needed to elucidate the exact signaling pathways. Although locomotor activity was not independently assessed using a dedicated locomotor test, total exploration time during the Novel Object Recognition test did not differ significantly among the experimental groups, indicating comparable baseline exploratory behavior. Therefore, the observed improvement in recognition memory is unlikely to be attributable to differences in exploratory activity alone. Nevertheless, future studies incorporating dedicated locomotor assessments would further strengthen the interpretation of the behavioral findings. Additionally, although the D-galactose model replicates certain features of aging, it does not fully capture the complexity of human neurodegeneration, which limits translational extrapolation. Lastly, the long-term sustainability of PBMT's therapeutic effects was not assessed in this study. Future work should address whether chronic or repeated LED exposure yields cumulative or persistent neuroprotective benefits.

6. Conclusion

This study shows that chronic exposure to 40-Hz LED photobiomodulation therapy alleviates cognitive and behavioral impairments, reduces oxidative stress and pro-inflammatory cytokines, and preserves hippocampal neuronal structure in a D-galactose-induced aging model. Although the precise molecular mechanisms remain to be clarified, these findings suggest that PBMT may exert neuroprotective effects relevant to aging-related decline. Further research is needed to investigate the underlying pathways, long-term efficacy, and clinical relevance of this approach.

Author Contribution

N.A.: Investigation, data analysis, writing original draft;

J.F-B.: resources; review

S.H.: supervision, resources, review;

M.N.: supervision, project administration, data analysis, writing-review and editing.

Funding

This article is based on a student thesis (Approval ID: IR.ARAKMU.AEC.1403.021) and the author would like to thank the Arak University of Medical Sciences, Arak, Iran, for their support, cooperation, and assistance throughout the study period.

Data Availability

Data and material are available upon request to the corresponding author.

Declarations;

Ethics Approval

All experiments were performed in accordance with the Guide for the Care and Use of Laboratory Animals (National Institutes of Health Publication No. 80–23, revised 1996). Additionally, all

experiments were conducted with the approval of the Research and Ethics Committee at Arak University of Medical Sciences (Approval ID: IR.ARAKMU.AEC.1403.021).

Consent to Participate

Not applicable.

Consent for Publication

Not applicable.

Competing Interests

The authors declare that they have no conflicts of interest.

Code availability

Not applicable.

References:

Almeida, A. J. P. O. d., Ribeiro, T. P., & Medeiros, I. A. d. (2017). Aging: molecular pathways and implications on the cardiovascular system. *Oxid. Med. Cell. Longev, 2017*(1), 7941563.

Antunes, M., & Biala, G. (2012). The novel object recognition memory: neurobiology, test procedure, and its modifications. *Cogn Process*, *13*(2), 93-110.

Aydın, A. F., Çoban, J., Doğan-Ekici, I., Betül-Kalaz, E., Doğru-Abbasoğlu, S., & Uysal, M. (2016). Carnosine and taurine treatments diminished brain oxidative stress and apoptosis in D-galactose aging model. *Metab Brain Dis*, *31*(2), 337-345.

Bartman, S., Coppotelli, G., & Ross, J. M. (2024). Mitochondrial dysfunction: a key player in brain aging and diseases. *Curr Issues Mol Biol*, *46*(3), 1987-2026.

Barzegar Behrooz, A., Aghanoori, M.-R., Nazari, M., Latifi-Navid, H., Vosoughian, F., Anjomani, M., Lotfi, J., Ahmadiani, A., Eliassi, A., & Nabavizadeh, F. (2024). 40 Hz light preserves synaptic plasticity and mitochondrial function in Alzheimer's disease model. *Sci Rep*, *14*(1), 26949.

Bradford, M. M. (1976). A rapid and sensitive method for the quantitation of microgram quantities of protein utilizing the principle of protein-dye binding. *Anal Biochem*, *72*(1-2), 248-254.

Çakatay, U. (2010). Protein redox-regulation mechanisms in aging. In *Aging and age-related disorders* (pp. 3-25). Springer.

Cardoso, F. d. S., de Souza Oliveira Tavares, C., Araujo, B. H. S., Mansur, F., Lopes-Martins, R. A. B., & Gomes da Silva, S. (2022). Improved spatial memory and neuroinflammatory profile changes in aged rats submitted to photobiomodulation therapy. *Cell Mol Neurobiol*, *42*(6), 1875-1886.

Cardoso, F. d. S., Salehpour, F., Coimbra, N. C., Gonzalez-Lima, F., & Gomes da Silva, S. (2022). Photobiomodulation for the treatment of neuroinflammation: A systematic review of controlled laboratory animal studies. *Front Neurosci*, *16*, 1006031.

Casanova, A., Wevers, A., Navarro-Ledesma, S., & Pruimboom, L. (2023). Mitochondria: It is all about energy. *Front Physiol*, *14*, 1114231.

Chen, C., Lin, X., Nguyen, V. P., Nong, Z., Li, W., Chen, Q., Ming, J., Xie, Q., & Huang, R. (2015). Yulangsan polysaccharide improves redox homeostasis and immune impairment in D-galactose-induced mimetic aging. *Food Funct*, *6*(5), 1712-1718.

Chen, P., Chen, F., & Zhou, B. (2018). Antioxidative, anti-inflammatory and anti-apoptotic effects of ellagic acid in liver and brain of rats treated by D-galactose. *Sci Rep*, *8*(1), 1465.

De Freitas, L. F., & Hamblin, M. R. (2016). Proposed mechanisms of photobiomodulation or low-level light therapy. *IEEE J Sel Top Quantum Electron*, *22*(3), 348-364.

Demirci-Çekiç, S., Özkan, G., Avan, A. N., Uzunboy, S., Çapanoğlu, E., & Apak, R. (2022). Biomarkers of oxidative stress and antioxidant defense. . *Pharm Biomed Anal*, *209*, 114477.

Eikelboom, W. S., Bertens, D., & Kessels, R. P. (2020). Cognitive rehabilitation in normal aging and individuals with subjective cognitive decline. In *Cognitive Rehabilitation and Neuroimaging: Examining the Evidence from Brain to Behavior* (pp. 37-67). Springer.

Godoy, J. A., Rios, J. A., Picón-Pagès, P., Herrera-Fernández, V., Swaby, B., Crepin, G., Vicente, R., Fernández-Fernández, J. M., & Muñoz, F. J. (2021). Mitostasis, calcium and free radicals in health, aging and neurodegeneration. *Biomol*, *11*(7), 1012.

Hamblin, M. R. (2016). Shining light on the head: Photobiomodulation for brain disorders. *BBA clinical*, *6*, 113-124.

Hamblin, M. R. (2019). Photobiomodulation for Alzheimer's disease: has the light dawned? Photonics,

Hashmi, J. T., Huang, Y. Y., Sharma, S. K., Kurup, D. B., De Taboada, L., Carroll, J. D., & Hamblin, M. R. (2010). Effect of pulsing in low-level light therapy. *Lasers Surg Med*, *42*(6), 450-466.

Heo, J.-C., Park, J.-A., Kim, D.-K., & Lee, J.-H. (2019). Photobiomodulation (660 nm) therapy reduces oxidative stress and induces BDNF expression in the hippocampus. *Sci Sep*, *9*(1), 10114.

Hosseini, L., Farazi, N., Erfani, M., Mahmoudi, J., Akbari, M., Hosseini, S. H., & Sadigh-Eteghad, S. (2022). Effect of transcranial near-infrared photobiomodulation on cognitive outcomes in D-galactose/AlCl3 induced brain aging in BALB/c mice. *Lasers Med Sci*, *37*(3), 1787-1798.

Iaccarino, H. F., Singer, A. C., Martorell, A. J., Rudenko, A., Gao, F., Gillingham, T. Z., Mathys, H., Seo, J., Kritskiy, O., & Abdurrob, F. (2016). Gamma frequency entrainment attenuates amyloid load and modifies microglia. *Nature*, *540*(7632), 230-235.

Ionescu-Tucker, A., & Cotman, C. W. (2021). Emerging roles of oxidative stress in brain aging and Alzheimer's disease. *Neurobiol Aging*, *107*, 86-95.

Islam, M. T. (2017). Oxidative stress and mitochondrial dysfunction-linked neurodegenerative disorders. *Neurol Res*, *39*(1), 73-82.

Jin, M., & Cai, S.-Q. (2023). Mechanisms underlying brain aging under normal and pathological conditions. *Neurosci Bull*, *39*(2), 303-314.

Karu, T. (1999). Primary and secondary mechanisms of action of visible to near-IR radiation on cells. *J Photochem Photobiol Biol*, *49*(1), 1-17.

López-Otín, C., Blasco, M. A., Partridge, L., Serrano, M., & Kroemer, G. (2023). Hallmarks of aging: An expanding universe. *Cell*, *186*(2), 243-278.

Maldonado, E., Morales-Pison, S., Urbina, F., & Solari, A. (2023). Aging hallmarks and the role of oxidative stress. *Antioxidants*, *12*(3), 651.

Mattson, M. P., & Magnus, T. (2006). Ageing and neuronal vulnerability. *Nat Rev Neurosci*, *7*(4), 278-294.

Nam, S. M., Seo, M., Seo, J.-S., Rhim, H., Nahm, S.-S., Cho, I.-H., Chang, B.-J., Kim, H.-J., Choi, S.-H., & Nah, S.-Y. (2019). Ascorbic acid mitigates D-galactose-induced brain aging by increasing hippocampal neurogenesis and improving memory function. *Nutrients*, *11*(1), 176.

Nazari, M., Jafari, A., Torabi, N., Vajed-Samiei, T., Ghasemi, R., Fahanik-Babaei, J., & Eliassi, A. (2022). The Effect of 40-Hz white LED therapy on structure–function of brain mitochondrial ATP-sensitive Ca-activated large-conductance potassium channel in amyloid beta toxicity. *Neurotox Res*, *40*(5), 1380-1392.

Nazari, M., Vajed-Samiei, T., Torabi, N., Fahanik-Babaei, J., Saghiri, R., Khodagholi, F., & Eliassi, A. (2022). The 40-Hz white light-emitting diode (LED) improves the structure–function of the brain mitochondrial KATP channel and respiratory chain activities in amyloid Beta toxicity. *Mol Neurobiol*, *59*(4), 2424-2440.

Pak, J. W., Herbst, A., Bua, E., Gokey, N., McKenzie, D., & Aiken, J. M. (2003). Mitochondrial DNA mutations as a fundamental mechanism in physiological declines associated with aging. *Aging Cell*, *2*(1), 1-7.

Rojas, J. C., & Gonzalez-Lima, F. (2013). Neurological and psychological applications of transcranial lasers and LEDs. *Biochem Pharmacol*, *86*(4), 447-457.

Rostami, F., Janahmadi, M., & Hosseinmardi, N. (2024). Aquaporin-4 inhibition attenuates Pentylenetetrazole-induced behavioral seizures and cognitive impairments in kindled rats. *Physiol Behav*, *278*, 114521.

Sadigh-Eteghad, S., Majdi, A., McCann, S. K., Mahmoudi, J., Vafaee, M. S., & Macleod, M. R. (2017). D-galactose-induced brain ageing model: a systematic review and meta-analysis on cognitive outcomes and oxidative stress indices. *PloS One*, *12*(8), e0184122.

Salehpour, F., Cassano, P., Rouhi, N., Hamblin, M. R., De Taboada, L., Farajdokht, F., & Mahmoudi, J. (2019). Penetration profiles of visible and near-infrared lasers and light-emitting diode light through the head tissues in animal and human species: a review of literature. *Photobiomodul, Photomed Laser Surg*, *37*(10), 581-595.

Schiffer, F., Johnston, A. L., Ravichandran, C., Polcari, A., Teicher, M. H., Webb, R. H., & Hamblin, M. R. (2009). Psychological benefits 2 and 4 weeks after a single treatment with near infrared light to the forehead: a pilot study of 10 patients with major depression and anxiety. *Behav Brain Funct*, *5*(1), 46.

Singer, A. C., Martorell, A. J., Douglas, J. M., Abdurrob, F., Attokaren, M. K., Tipton, J., Mathys, H., Adaikkan, C., & Tsai, L.-H. (2018). Noninvasive 40-Hz light flicker to recruit microglia and reduce amyloid beta load. *Nat Protoc*, *13*(8), 1850-1868.

Soleimani, E., Ahmadiani, A., Bazrgar, M., Khodagholi, F., & Eliassi, A. (2024). The 40-Hz white light emitting diode to alleviate psychiatric symptoms induced by streptozotocin in vivo. *Basic Clin Neurosci*, *15*(4), 463.

Speisman, R. B., Kumar, A., Rani, A., Foster, T. C., & Ormerod, B. K. (2013). Daily exercise improves memory, stimulates hippocampal neurogenesis and modulates immune and neuroimmune cytokines in aging rats. *Brain Behav Immun*, *28*, 25-43.

Sun, X., Jiao, X., Ma, Y., Liu, Y., Zhang, L., He, Y., & Chen, Y. (2016). Trimethylamine N-oxide induces inflammation and endothelial dysfunction in human umbilical vein endothelial cells via activating ROS-TXNIP-NLRP3 inflammasome. *Biochem Biophy Res Commun*, *481*(1-2), 63-70.

Turgut, N. H., Mert, D. G., Kara, H., Egilmez, H. R., Arslanbas, E., Tepe, B., Gungor, H., Yilmaz, N., & Tuncel, N. B. (2016). Effect of black mulberry (Morus nigra) extract treatment on cognitive impairment and oxidative stress status of D-galactose-induced aging mice. *Pharm Biol*, *54*(6), 1052-1064.

Vatansever, F., & Hamblin, M. R. (2012). Far infrared radiation (FIR): Its biological effects and medical applications: Ferne Infrarotstrahlung: Biologische Effekte und medizinische Anwendungen. *Photon Laser Med*, *1*(4), 255-266.

Vina, J., Borras, C., Abdelaziz, K. M., Garcia-Valles, R., & Gomez-Cabrera, M. C. (2013). The free radical theory of aging revisited: the cell signaling disruption theory of aging. *Antioxid Redox Signal*, *19*(8), 779-787.

Xu, L.-Q., Xie, Y.-L., Gui, S.-H., Zhang, X., Mo, Z.-Z., Sun, C.-Y., Li, C.-L., Luo, D.-D., Zhang, Z.-B., & Su, Z.-R. (2016). Polydatin attenuates d-galactose-induced liver and brain damage through its anti-oxidative, anti-inflammatory and anti-apoptotic effects in mice. *Food Funct*, *7*(11), 4545-4555.